

# Effects of Polysulfone (PSf) Support Layer on the Performance of Thin-Film Composite (TFC) Membranes

Chuan Ding<sup>1</sup>, Jun Yin<sup>2</sup>, Baolin Deng<sup>1,2\*</sup>

<sup>1</sup>Department of Chemical Engineering, University of Missouri, Columbia, MO 65211, USA

<sup>2</sup>Department of Civil & Environmental Engineering, University of Missouri, Columbia, MO 65211, USA

\*Corresponding author: Baolin Deng, Department of Civil & Environmental Engineering, University of Missouri, Columbia, MO 65211, USA; Tel: +1 573 882 0075; E-mail: dengb@missouri.edu

Received Date: September 07, 2014 Accepted Date: November 11, 2014 Published Date: November 13, 2014

Citation: Baolin Deng (2014) Effects of Polysulfone (PSf) Support Layer on the Performance of Thin-Film Composite (TFC) Membranes. J Chem Proc Eng 1: 1-8.

## Abstract

The performance of thin-film composite (TFC) membranes was related to the properties of support layers. In this study, polysulfone (PSf) membranes formed by the phase inversion process under various concentrations of PSf and polyvinylpyrrolidone (PVP) additive were used as support layers to prepare polyamide (PA) TFC membranes by the interfacial polymerization (IP). The effects of PSf and PVP concentrations on the properties of support layer such as equilibrium water content (EWC), pure water flux, and molecular weight cut off (MWCO) were investigated. And the performance of resulting TFC membranes was evaluated in terms of water flux and salt rejection. The pure water flux decreased with increasing PSf concentration in support layers. The decrease of water flux could be attributed to a lower effective area of PA when a denser support layer was used. The addition of PVP in the casting solution resulted in a more porous and hydrophilic support layer. However, the water flux of TFC membranes decreased which could be due to the larger effective thickness of PA.

**Keywords:** Thin film composite membrane; Polysulfone support layer; Polyvinylpyrrolidone; Interfacial polymerization; Water flux

## Introduction

Reverse osmosis (RO) is a common method to remove dissolved salts from seawater and brackish water [1]. Water flux and salt rejection are two key parameters for RO membranes, and efficient desalination relies on both high water flux and salt rejection of the membrane. The thin-film composite (TFC) membranes are widely used in commercial single pass seawater desalination plants because they exhibit high water flux and salt and organic rejections, a wide operating range of temperature and pH, and high stability to biological attacks [2-5]. The TFC membranes consist of a highly-selective thin aromatic polyamide (PA) layer formed via in situ polycondensation on a reinforced porous sublayer. A great advantage of TFC technology is that the ultra-thin barrier layer and the porous support can be independently optimized with respect to structure, stability, and performance [6].

Porous support layers are commonly prepared by the phase separation of polymer solution [7]. Numerous studies have been carried out to investigate the effects of polymer concentration and additives on the performance of this porous sup-

port membrane. It is well known that the polymer concentration in the casting solution has a great effect on the porosity of the final membrane [8]. A higher polymer concentration will lead to a lower porosity, because increasing the polymer concentration in solution results in a higher viscosity, thus reducing transport rates and slowing the demixing process [9]. A higher polymer concentration has also shown to increase the membrane top layer thickness and decrease formation of macrovoid [10]. Another important parameter is the additive in the casting solution, which can affect the final membrane characteristics either by changing solvent capacity or by changing phase separation kinetics and thermodynamic properties [11]. The most important effects of the additives are the increase of hydrophilicity of the membrane surface, suppression of macrovoid formation, and enhancement of pore interconnectivity [12]. Polyvinylpyrrolidone (PVP) was usually used as the additive in the preparation of porous polysulfone (PSf) or polyethersulfone (PES) membranes for ultrafiltration (UF). The addition of PVP showed various effects on porous membrane structure originating from different dope solution compositions. For example, the work of Boom showed that PVP suppressed the formation of macrovoid in the substrate layer in PES/N-methylpyrrolidone (NMP)/PVP solution [12]. In another study, Yoo and et al.

©2013 The Authors. Published by the JScholar under the terms of the Creative Commons Attribution License <http://creativecommons.org/licenses/by/3.0/>, which permits unrestricted use, provided the original author and source are credited.

[13] indicated that PVP enlarged the macrovoid structure rather than suppressed the pore structure in PSf/ Dimethylformamide (DMF)/PVP solutions. All these effects could further influence the performance of final TFC membranes.

Fabrication of the thin barrier layer is based on interfacial polymerization (IP), i.e., a polymerization reaction that takes place at the interface of porous support layer between two immiscible phases [14]. Usually, the thin-film active layer consists of aromatic PA formed by the IP of *m*-phenylenediamine (MPD) in the aqueous phase and trimesoyl chloride (TMC) in the organic phase. Two structural moieties may exist in the derived PA. One is the crosslinked portion (*m*) and the other is the linear moiety (*n*), which has an unreacted acid chloride groups that subsequently hydrolyzes to form a carboxylic acid group.

There are many studies reported in the literature on the impact of polymer concentration and additive to the structure and performance of UF membranes. It is not clear, however, how the changing characteristics of the support layer, including those induced by using different polymer concentrations and additive during the fabrication process, could affect the performance of the TFC membranes. In this work, we aimed to evaluate the effects of polymer concentration and additive on the support layer formation and in particular, the performance of the TFC membranes fabricated using support layers of varying characteristics.

## Experimental

### Materials

PSf beads (35,000 Da), PVP powder (10,000 Da and 40,000 Da), DMF (anhydrous, 99.8%), TMC (98%), MPD (99.8%), Red MX-5B (615.33 Da), and Bovine serum albumin (BSA, 66,000 Da) were purchased from Sigma-Aldrich (St. Louis, MO) and used as received.

### Preparation of PSf porous support layers

A measured amount of PSf was added to airtight bottles and then a specified amount of DMF was added to dissolve the PSf. When the effects of the PVP additive were studied, the polymer-solvent mixture was also spiked with a specified amount of PVP. This casting solution was ultrasonicated for 1 h and stirred at 45 °C for 6 h. And then, the casting solution was kept still overnight at room temperature for degassing. The membrane was formed by spreading the polymer solution over a clean glass plate by a casting knife with a gap of 100µm followed by immediately immersing the glass plate into the deionized (DI) water at room temperature. The precipitated membrane was washed thoroughly and stored in DI water at 5 °C prior to test.

Various porous support membranes were produced by systematically changing the casting solutions. The effect of PSf concentration was studied by varying PSf from 11 to 19 wt% in DMF solvent, while the influence of additive PVP was studied by keeping PSf concentration fix at 15 wt% and varying PVP from 1 to 10 wt% in the total dope solution.

### TFC membrane fabrication

The PA thin-film layer was formed on the top of the PSf support membranes via IP process. Briefly, 2 % MPD in DI water and 0.15 % TMC in hexane were used. The PSf substrate layer, placed on a glass plate, was immersed in 2 % MPD solution. After 5 min, the excess MPD was removed by using a rubber roller and then 0.15 % TMC hexane solution was dripped on the surface to react with MPD for 120 s, which led to the formation of an active skin layer over the PSf support. The membrane was then post-treated at 80 °C for 5 min and stored in DI water at 5 °C prior to the performance testing.

### Characterizations and performance assessment of support layers

The hydrophilicity of substrate membrane can be evaluated by using water contact angle as a proxy. In the present study, the water contact angles of membranes were measured by the sessile drop method on a video contact angle system (VCA-2500 XE, AST products, Billerica, MA).

Equilibrium water content (EWC) is related to the porosity of a membrane. It is an important parameter as it indirectly indicates the degree of hydrophilicity or hydrophobicity of a membrane [15]. Membranes were weighed in an electronic balance in a wet state after mopping the surface water with a clean tissue paper. The wet membranes were dried in an oven for 2 h at 60 °C and weighed. The EWC at room temperature was calculated as follows:

$$EWC = \frac{W_w - W_d}{W_w} \times 100\% \quad (1)$$

where  $W_w$  is weight of wet membranes (g) and  $W_d$  weight of dry membranes (g).

The scanning electron microscope (SEM) images were collected for the top surfaces as well as cross-sections of membranes by using Quanta FEG 600 (FEI Company, Hillsboro, OR). The specimen was coated with platinum by a sputter coater (K575x, Emitech Ltd., Kent, England) at 20 mA for 1 min to increase conductivity. To obtain the cross section images, the wet membranes were cut into pieces and were immersed in liquid nitrogen. The frozen membranes were then broken by tweezers to avoid the structure damage in the cross-section.

To assess the support membrane, a dead-end test system was used for measuring pure water flux and molecular weight cut off (MWCO). The filtration set-up was described in our previous study [16], where the membrane holder (Stirred cell 8200, Millipore Corp.) had an effective membrane area of 28.7 cm<sup>2</sup>. To eliminate the influence of membrane compaction, membranes were pre-compacted at 20 psi for 2 h, by which time a steady-state flux was observed. The water flux was calculated as the following equation:

$$J_w = \frac{Q}{A\Delta t} \quad (2)$$

where  $J_w$  is the pure water flux (L/m<sup>2</sup>h),  $Q$  the volume of water permeated (L),  $A$  the effective membrane area (m<sup>2</sup>), and  $\Delta t$  the permeation time (h).

The MWCO of a membrane is generally defined as the molecular weight of a solute at which above 90% of the solute is retained. In the present study, chemicals of different molecu-

lar weights including Red MX-5B (615.33 Da), PVP (10 kDa), PVP (40 kDa) and BSA (66 kDa) were chosen to test solute rejection and MWCO. The BSA was prepared at a concentration of 1000 mg/L in PBS buffer (pH 7.4) and the others were prepared at a concentration of 1000 mg/L in the ultrapure water. The membrane holder was filled with solution and pressurized at a constant pressure of 10 psi and stirred at 200 rpm throughout the experiments to minimize concentration polarization. During the filtration, the permeate solutions were collected over a period of time. Red MX-5B and BSA concentrations were measured by using a UV-visible spectrophotometer at a wavelength of 530 nm and 280 nm, respectively. PVP (10 kDa or 40 kDa) concentrations were analyzed by a TOC analyzer (TOC-5000, Shimadzu Corp., Japan). The solute rejection was calculated by using Eq. 3.

$$R = 1 - \left( \frac{C_p}{C_f} \right) \times 100\% \quad (3)$$

where  $C_p$  and  $C_f$  are permeate concentration and feed concentration, respectively.

### Characterizations and performance assessment of TFC membranes

The surface morphology of TFC membrane was analyzed by SEM. The sample preparation procedure was the same as that of the substrate membrane. The functional groups of membrane surface were identified by attenuated total reflection Fourier transform infrared (ATR FT-IR) spectroscopy. Nicolet 4700 FT-IR (Thermo Electron Corporation, Waltham, MA) equipped with multi-reflection Smart Performers ATR accessory was used for this analysis. All spectra included the wave numbers from 650 to 4000  $\text{cm}^{-1}$  with 64 scans at a resolution of 2.0  $\text{cm}^{-1}$ .

The performance of TFC membranes were evaluated by a high pressure filtration system as presented in our pervious study [17]. The membrane holder (Model: XX4504700, stainless steel, Millipore Corp., Billerica, MA) had an effective membrane area of 9.6  $\text{cm}^2$ . Prior to test, each membrane was compressed by DI water at 300 psi for 5 h. After pure water flux test, salt solution (final concentration of 2000 mg/L of NaCl) was added and the conductivity of feed and permeate solutions was measured by a conductivity/TDS meter (HACH Company, Loveland, CO). The measurement was conducted at  $25 \pm 1$   $^\circ\text{C}$ , which was controlled by a water circulator (Isotemp 6200 R20F, FisherScientific, Inc., Pittsburgh, PA). The pure water flux and salt rejection were calculated with Eq. (4) and Eq. (5), respectively.

$$J = \frac{0.001M}{A * \left( \frac{t}{3600} \right) * P} \quad (4)$$

$$R = \left( 1 - \frac{C_p}{C_f} \right) \times 100\% \quad (5)$$

where  $J$  is the water flux ( $\text{L}/\text{m}^2\text{h}$ ),  $M$  is the weight of permeate (g),  $A$  is the effective membrane area ( $\text{m}^2$ ),  $t$  is the test time (s),  $P$  is the applied pressure (psi),  $R$  is the rejection ratio and  $C_p$  and  $C_f$  are the concentration of permeate and feed solution, respectively.

## Results and discussion

### Effects of PSf concentration on support layers

Cross-sectional and surface morphologies of support layers and surfaces of TFC membranes were obtained through SEM analysis and presented in Figure 1. In the cross-sectional images, a typical asymmetric structure was observed. The finger-like macrovoids were suppressed with increasing PSf concentration. Furthermore, when PSf concentration reached 19%, the structure became sponge-like and appeared much denser compared with support layer with 11% PSf. In general, increasing the polymer concentration in casting solution would result in a higher viscosity, which tends to reduce transport rates thereby produce a slower demixing [9]. Furthermore, the precipitation path will cross the binodal at a higher polymer concentration. These factors could contribute to a thicker top layer, lower porosity and diminished macrovoid formation [10].

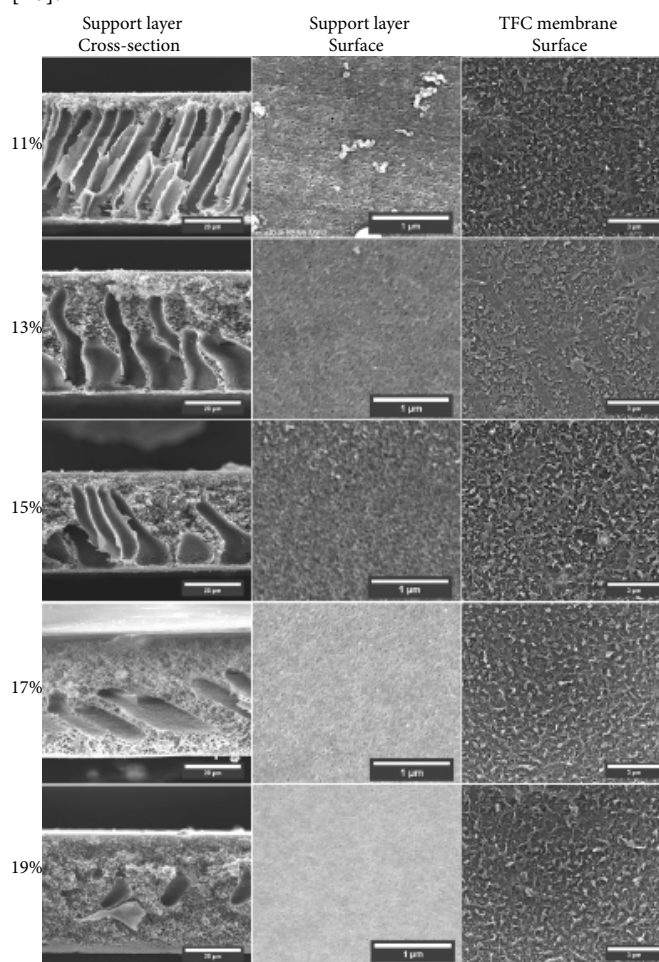


**Figure 1:** SEM images from cross-sections and surfaces of membranes with different PSf concentrations.

The pore information for each support layer calculated by software Image J was presented in Table 1 (images with higher resolution were presented in Fig. S1), including the average pore size and pore area fraction of the support layers.

The pore area fraction decreased with increasing PSf concentration. This is consistent with the previous result that the substrate membrane became denser and less porous when the PSf concentration was high. For TFC membrane surface, a typical

**Table 1:** Pore size and area fraction of membranes with different PSf concentrations

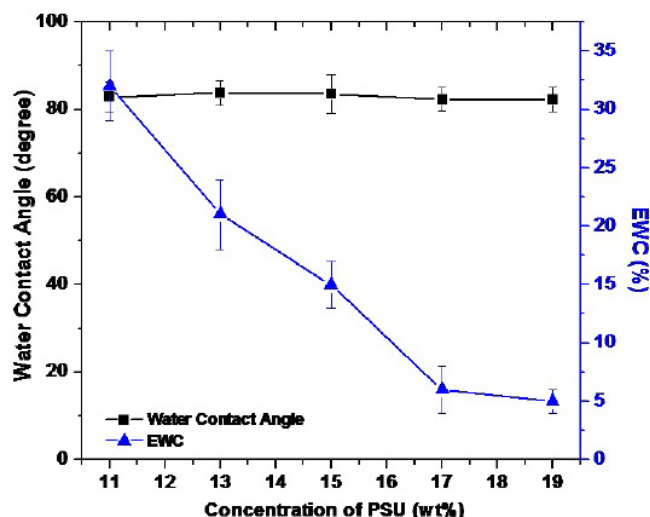
PSf Concentration (wt%)	Average Pore Size (nm)	Area Fraction(%)
11%	14.9	2.7
13%	14.5	1.8
15%	15.2	2.5
17%	12.4	1.4
19%	11.4	1.1

“ridge and valley” morphology was observed. There is no obvious difference between PA layers formed on different support layers.

Water contact angle can be used as a method to test the hydrophilicity of substrate membranes. As indicated by Figure 2, there was no significant change in the water contact angle among membranes prepared with different PSf concentrations. The contact angle was around 83° for all support layers. It appeared that while there were some structural changes in morphology of the membranes, the membrane hydrophilicity as indicated by the contact angle measurements remained the same, suggesting that here the hydrophilicity was mainly controlled by the polymer chemistry.

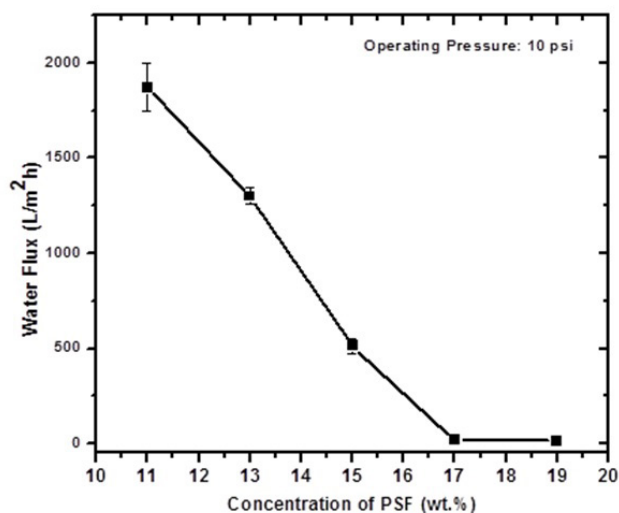
EWC of the membrane, however, decreased significantly with increasing PSf concentration (Figure 2). The decrease in EWC confirmed the change of porosity in the support layer with increasing PSf concentration, because the surface pores as well as cavities inside the support layer are responsible for accommodating water in the membranes [18].

The support layers were further assessed for their pure wa-

**Figure 2:** Water contact angles and water uptakes of support layers prepared with different PSf concentrations.

ter flux and MWCO. Figure 3 indicated that the pure water flux, measured under the pressure of 10 psi, decreased with increasing PSf concentration. The water flux was minimal for membranes prepared from 17% and 19% PSf. This is consistent with the SEM results of membrane surfaces and cross-sections, where higher PSf concentration led to a denser layer with thicker skin layer and smaller surface pores.

The membrane MWCOs were assessed by measuring rejections of solutes with different molecular weights, using the

**Figure 3:** Water fluxes of support layers prepared with different PSf concentrations.

dead-end system under a trans-membrane pressure of 10 psi. As shown in Figure 4, the MWCO decreased with increasing PSf concentration. This is consistent with our general understanding that the support layer became denser and less porous when the PSf concentration was high, which would lead to a high solute rejection.

#### Effects of PVP concentration on support layers

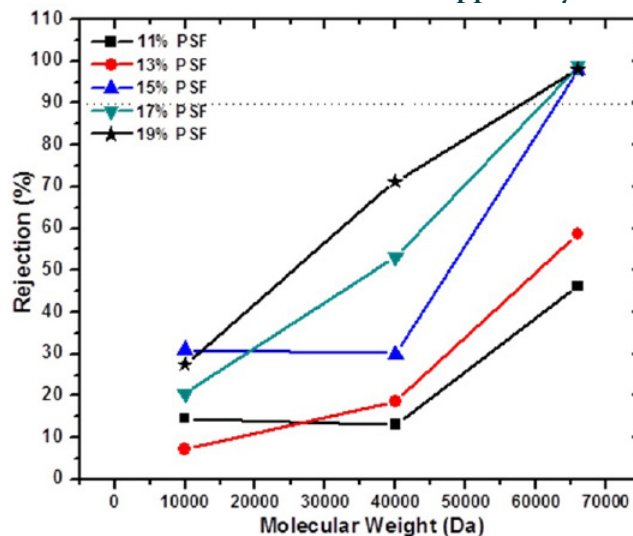
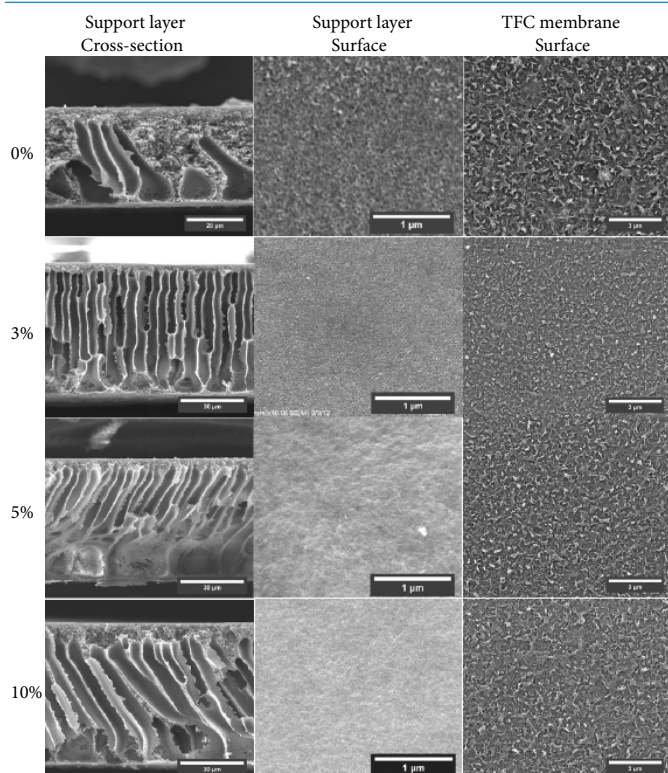
**Figure 4:** Solute rejections of support layers prepared with different PSf concentrations.

Figure 5 presents the SEM images of support layers and TFC membranes prepared with different PVP concentrations. Similarly, they showed an asymmetric structure consisting of a dense top layer and a porous sublayer. The sublayer seems to have finger-like cavities as well as macrovoid structure. For macrovoid formation, the membrane must have a skin layer to limit the penetration of a large amount of nonsolvent into the sublayer and must prevent nuclei formation after a few nuclei (which were the origins of the macrovoids) formed [19]. PVP is likely to be leached out from the membrane and the structure growth rate increased with PVP, leading to the formation of the porous layer. When the PVP concentration increased, however, the growth rate became slower, so the top layer became thicker again.

For the surface of support layers, the membranes were quite



**Figure 5:** SEM images from cross-sections and surfaces of membranes with different PVP concentrations.

porous at 0% PVP and 3% PVP. With further increasing PVP concentration to 5% and 10%, the surface became denser and less porous. This could be attributed to the diffusion rate of solvent. When PVP concentration was low, the polymer diffusion rate is high, making the surface more porous. However, when PVP concentration reached 5%, the viscosity played a dominant role in the diffusion process. Low diffusion rate made the support layer surface less porous. For TFC membrane surfaces, there is no obvious difference in polyamide layer surface morphology among the supports with different PVP concentrations.

For support layers with different PVP concentrations (Table 2: Pore size and area fraction of membranes with different PVP concentrations

PVP Concentration (wt%)	Average Pore Size (nm)	Area Fraction (%)
0%	15.2	2.5
3%	13.5	3.2
5%	12.6	1.5
10%	10.6	1.2

2, images with higher resolution were presented in Fig. S2), the area fraction increased when PVP concentration increased to 3%, then it decreased with further increasing PVP concentration. This result is consistent with the previous observation about the trade-off correlation between the thermodynamic enhancement and rheological diffusion inhibition.

As shown in Figure 6, water contact angle of the support membranes decreased from  $83.6 \pm 4.5^\circ$  to  $34.5 \pm 10.8^\circ$  with increasing PVP concentration, indicating an increased surface hydrophilicity. The water contact angle of membrane with 10% PVP was not shown here because after dropping water droplet on

membrane surface, it spread too fast to measure a stable water contact angle.

Furthermore, EMC increased with increasing PVP concentra-

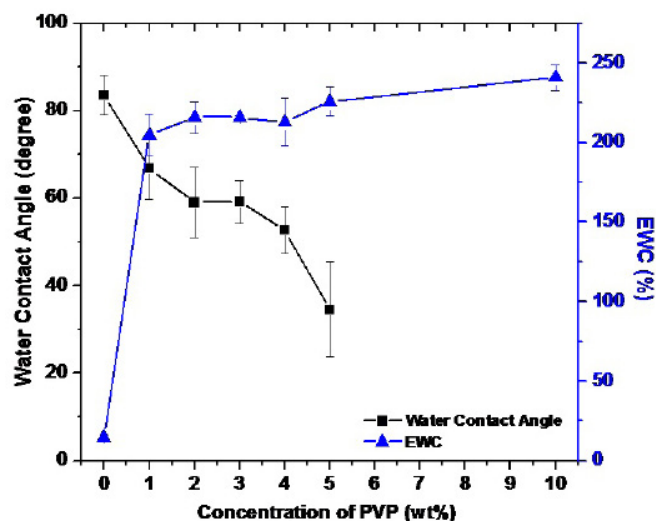


**Figure 6:** Water contact angles and water uptakes of support layers prepared with different PVP concentrations.

tion. Even introducing 1% PVP into the casting solution could increase EMC significantly. PVP increased the porosities and enlarged the pore size, which would cause more water entrapped inside the support layer.

Figure 7 presents the pure water flux for support layers containing various PVP concentrations. The pure water flux increased initially with increasing PVP concentration, however, when the PVP concentration reached 4%, it started to decrease. The fluxes of membranes with 5% PVP and 10% PVP were even lower than the one without PVP.

For UF or microfiltration (MF) membranes, the pore size and

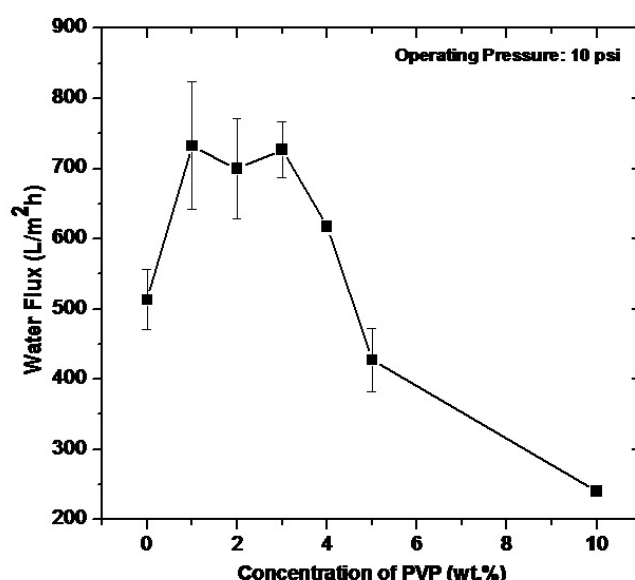


**Figure 7:** Water fluxes of support layers prepared with different PVP concentrations.

pore distribution on the dense layer determine the water flux. Here, the initial increase of water flux can be explained by the enhanced phase separation induced by the thermodynamic immiscibility of PVP. The decrease of water flux with a PVP concentration over 4% could be attributed to the hindered

molecular diffusion induced by the increased viscosity after introducing PVP. At a low PVP concentration, the enhancement of phase separation could outweigh the hindered diffusion. The increased demixing rate on the interface induced the rapid collapse of polymer molecules concurrent with the formation of gaps between collapsed molecules, leading to a more porous and permeable membrane [20, 21]. With a further increase of PVP concentration, diffusion delay due to the increased viscosity could overcome the enhancement of phase separation, leading to a dense and thick top layer with low porosity and low degree of pore interconnectivity [22]. Therefore, the convex relationship between water flux and PVP concentration can be explained by the trade-off relationship between the thermodynamic immiscibility and rheological diffusion inhibition. Similarly, when the oxidized multi-walled carbon nanotubes (OMWNTs)/PSf nanocomposite hollow fiber membranes were developed [23], we also observed a convex relationship between water flux and filler concentration. The hydrophilic OMWNTs played a similar role as PVP during the phase separation process.

Figure 8 shows the rejections of different solutes by support membranes prepared with different PVP concentrations. There was no clear trend for the change of MWCO with increasing PVP concentration. However, when compared with the MWCO of support layer containing 0% PVP presented in Figure 4 (15% PSf), the addition of PVP was found to have changed the MWCO to some extent.

### Performance of TFC membranes

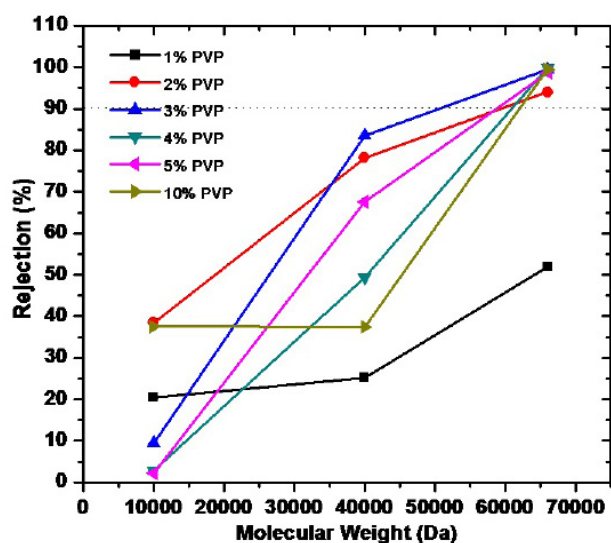


**Figure 8:** Solute rejections of support layers prepared with different PVP concentrations.

TFC membranes prepared with different support layers were examined to study the effects of support layer properties on the permeation behavior of TFC membranes. The membranes were characterized in terms of water flux and salt rejection.

As presented in Figure 9, the water flux decreased with increasing PSf concentration, while salt rejection increased at first and leveled off. Considering the unchanged surface hydrophilicity of support layers, the changed flux could be attributed to the porous support layer with more water channels which can collect permeate from the PA thin-film layer. So the effectiveness of PA thin-film layer seemed to increase with more open

support layer structure. The relatively low salt rejection ( $87 \pm 1.5 \text{ L/m}^2\text{h}$ ) for TFC membrane prepared with low PSf concentration (11 %) could be caused by the existence of small defects on the loose support layer after IP process. With an increase of PSf concentration to 15 %, the salt rejection reached 97.5 %, the water flux decreased from 40 to 30  $\text{L/m}^2\text{h}$ , though. As presented in Figure 10, salt rejection maintained a high val-

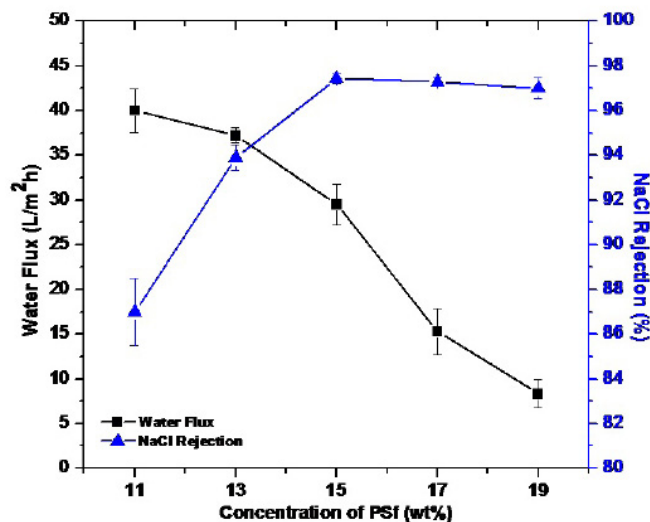


**Figure 9:** Water fluxes and salt rejections of TFC membranes with supports prepared with different PSf concentrations.

ue of 97.5%, however, the water flux decreased with increasing PVP concentration. Ghosh and Hoek [24] found that hydrophobic and rough support membranes produced PA composites with a higher water permeability because less PA was introduced to the inside pores so the diffusion pass of water was not significantly increased. Our observations were consistent with the literature reports. With an increasing hydrophilicity of support layer, the water permeation decreased, demonstrating that the support layer hydrophilicity was an important factor during the IP process. It was reported that hydrogen bonding between MPD and hydrophilic substrates limited the diffusion rate of MPD inside the pores of support layer. In this situation, some TMC may diffuse into the pores and form PA deep inside the pores creating a longer effective film thickness for water permeation [25, 26]. That's why pure water flux could be higher for PA composites formed over support layers which were a little bit hydrophobic. However, highly hydrophobic support layer was not suitable for making PA TFC. To illustrate, we had to modify the surface of polyvinylidene difluoride (PVDF) membrane by plasma treatment to fabricate PVDF-supported TFC membranes [16].

In order to further characterize the thickness of PA thin-film layer, ATR-FTIR spectroscopy technique was used to identify the main functional groups of the PA thin-film layer and thereby estimate its thickness based on the calculated depth of penetration ( $d_p$ ) of infrared beam into the sample material and absorbance of the carbonyl-stretching characteristic band pertaining to amide linkage [27]. The spectra of TFC membranes prepared with different support layers are given in Figure 11a. The spectra indicated that the IP process had occurred since a strong band at  $1660 \text{ cm}^{-1}$  (amide I) was present which is the characteristic peak of the C=O band of an amide group. Other characteristic peaks of PA were also observed at  $1547 \text{ cm}^{-1}$

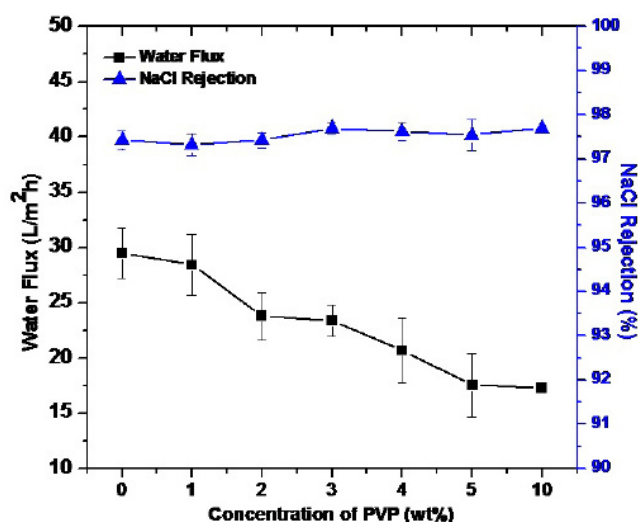


**Figure 10:** Water fluxes and salt rejections of TFC membranes with supports prepared with different PVP concentrations.

(amide II, C-N stretch) and  $1610\text{ cm}^{-1}$  (aromatic ring breathing) [28]. By comparing the peak intensity, we were able to roughly estimate and compare the effective thickness of PA in different TFC membranes.

During the calculation, all FTIR spectra were adjusted to the

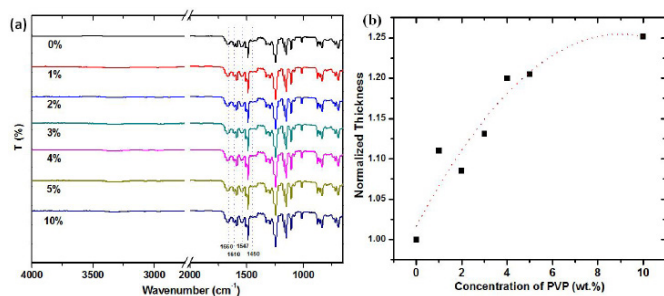


**Figure 11:** ATR-FTIR spectra of the TFC membranes prepared on support layers with different PVP concentrations (a) and normalized thickness of PA thin-film layer (b).

same baseline, and then the absorbance intensities of all peaks located at  $1660\text{ cm}^{-1}$  were recorded and the values are 2.68, 2.98, 2.91, 3.04, 3.22, 3.24, and 3.36 for membranes with PVP concentrations from 0 to 10%, respectively. Although, the actual thicknesses of PA thin-film layers could not be obtained without testing the intensity from a standard PA sample of known thickness, the normalized thicknesses could be calculated by dividing all the values with 2.68 as shown in Figure 11b. The thickness increased with increasing PVP concentration. This is consistent with our previous assumption that the effective thickness of PA thin-film layer became larger with increasing support layer hydrophilicity.

## Conclusion

In this work, a series of support layers were fabricated by casting solutions containing different PSf and PVP concentrations through phase inversion method. And then the performances of TFC membranes prepared based on these support layers were systematically studied to elucidate the correlation between support layer properties and TFC membrane performance. The results showed that increasing the PSf concentration in the PSf/DMF system changed the cross-sectional structure of support layer from an asymmetric whole finger

type to sponge type structure. Meanwhile, the support layer showed a less porous surface, lower water uptake and lower water permeability. The water permeability of resulting TFC membranes decreased with increasing PSf concentration because of low porous support layer structure.

In PSf/PVP/DMF system, PSf concentration was maintained at 15 wt%. The PVP with an average molecular weight of 10 kDa was used as an additive. Results showed that with an increase of PVP concentration in casting solution: (i) the cross-sectional morphology of support layer changed from sponge-like to finger-like; (ii) the surface hydrophilicity increased; (iii) the EWC increased which may result from the increased porosity of support layer; (iv) the water flux of resulting TFC membrane decreased due to the increased thickness of PA thin-film layer, while the salt rejection remained relatively high.

## Acknowledgments

We gratefully acknowledge Professor Qingsong Yu in the Department of Mechanical & Aerospace Engineering at MU for providing us access to the video contact angle measurement system. Financial support of this research was partially supported by the United Geological Survey through Missouri Water Resources Research Center.

## References

- 1) MG Marcovecchio, SF Mussati, PA Aguirre, J Nicolás (2005) Optimization of hybrid desalination processes including multi stage flash and reverse osmosis systems. *Desalination* 182: 111-122.
- 2) RJ Petersen (1993) Composite reverse osmosis and nanofiltration membranes. *Journal of Membrane Science* 83: 81-150.
- 3) T Younos, KE Tulou (200) Overview of desalination techniques. *Journal of Contemporary Water Research & Education* 132: 3-10.
- 4) M Wethern, W Katzaras (1995) Reverse osmosis treatment of municipal sewage effluent for industrial reuse. *Desalination* 102: 293-299.
- 5) T Asano (1998) Waste water reclamation and reuse. CRC, 1998.
- 6) BH Jeong, E Hoek, Y Yan, A Subramani, X Huang (2007) Interfacial polymerization of thin film nanocomposites: A new concept for reverse osmosis membranes. *Journal of Membrane Science* 294: 1-7.
- 7) M Mulder (1996) Basic principles of membrane technology. Springer. 2nd edn: 64p.
- 8) C Tam, T Tweddle, O Kutowy, . Hazlett (1993) Polysulfone membranes II. Performance comparison of polysulfone-poly-(N-vinylpyrrolidone) membranes. *Desalination* 89: 275-287.
- 9) C Smolders, A Reuvers, R Boom, I Wienk (1992) Microstructures in phase-inversion membranes. Part 1. Formation of macrovoids. *Journal of Membrane Science* 73: 259-275.
- 10) P Van de Witte, P Dijkstra, J Van den Berg, J Feijen (1996) Phase separation processes in polymer solutions in relation to membrane formation. *Journal of Membrane Science* 117: 1-31.
- 11) P Machado, A Habert, C Borges (1999) Membrane formation mechanism based on precipitation kinetics and membrane morphology: flat and hollow fiber polysulfone membranes. *Journal of Membrane Science* 155: 171-183.
- 12) R Boom, I Wienk, T Van den Boomgaard, C Smolders (1992) Microstructures in phase inversion membranes. Part 2. The role of a polymeric additive. *Journal of Membrane Science* 73: 277-292.

13) SH Yoo, JH Kim, JY Jho, J Won, YS Kang (2004) Influence of the addition of PVP on the morphology of asymmetric polyimide phase inversion membranes: effect of PVP molecular weight. *Journal of Membrane Science* 236: 203-207.

14) A Korikov, P Kosaraju, K Sirkar (2006) Interfacially polymerized hydrophilic microporous thin film composite membranes on porous polypropylene hollow fibers and flat films. *Journal of Membrane Science* 279: 588-600.

15) B Chakrabarty, A Ghoshal, M Purkait (2008) Effect of molecular weight of PEG on membrane morphology and transport properties. *Journal of Membrane Science* 309: 209-221.

16) ES. Kim, YJ Kim, Q Yu, B Deng (2009) Preparation and characterization of polyamide thin-film composite (TFC) membranes on plasma-modified polyvinylidene fluoride (PVDF). *Journal of Membrane Science* 344: 71-81.

17) J Yin, ES. Kim, J Yang, B Deng (2012) Fabrication of a novel thin-film nanocomposite (TFN) membrane containing MCM-41 silica nanoparticles (NPs) for water purification. *Journal of Membrane Science* 423-424: 238-246.

18) M Sivakumar, R Malaisamy, C Sajitha, D Mohan, V Mohan, et al. (1999) Ultrafiltration application of cellulose acetate-polyurethane blend membranes. *European polymer journal* 35: 1647-1651.

19) JH Kim, KH Lee (1998) Effect of PEG additive on membrane formation by phase inversion. *Journal of Membrane Science* 138: 153-163.

20) MJ Han, ST Nam (2002) Thermodynamic and rheological variation in polysulfone solution by PVP and its effect in the preparation of phase inversion membrane. *Journal of Membrane Science* 202: 55-61.

21) KW Lee, BK Seo, ST Nam, MJ Han (2003) Trade-off between thermodynamic enhancement and kinetic hindrance during phase inversion in the preparation of polysulfone membranes. *Desalination* 159: 289-296.

22) P Van De Witte, PJ Dijkstra, JWA Van Den Berg, J Feijen (1996) Phase separation processes in polymer solutions in relation to membrane formation. *Journal of Membrane Science* 117: 1-31.

23) J Yin, G Zhu, B Deng (2013) Multi-walled carbon nanotubes (MWNs)/polysulfone (PSU) mixed matrix hollow fiber membranes for enhanced water treatment. *Journal of Membrane Science*, 437: 237-248.

24) AK Ghosh, EMV Hoek (2009) Impacts of support membrane structure and chemistry on polyamide-polysulfone interfacial composite membranes. *Journal of Membrane Science* 336: 140-148.

25) Y Song, F Liu, B Sun (2005) Preparation, characterization, and application of thin film composite nanofiltration membranes. *Journal of Applied Polymer Science* 95: 1251-1261.

26) M Fathizadeh, A Aroujalian, A Raisi (2012) Effect of lag time in interfacial polymerization on polyamide composite membrane with different hydrophilic sub layers. *Desalination* 284: 32-41.

27) A Prakash Rao, S Joshi, J Trivedi, C Devmurari, V Shah (2003) Structure-performance correlation of polyamide thin film composite membranes: effect of coating conditions on film formation. *Journal of Membrane Science* 211: 13-24.

28) HA Shawky, SR Chae, S Lin, MR Wiesner (2011) Synthesis and characterization of a carbon nanotube/polymer nanocomposite membrane for water treatment. *Desalination* 272: 46-50.

## Support Figures

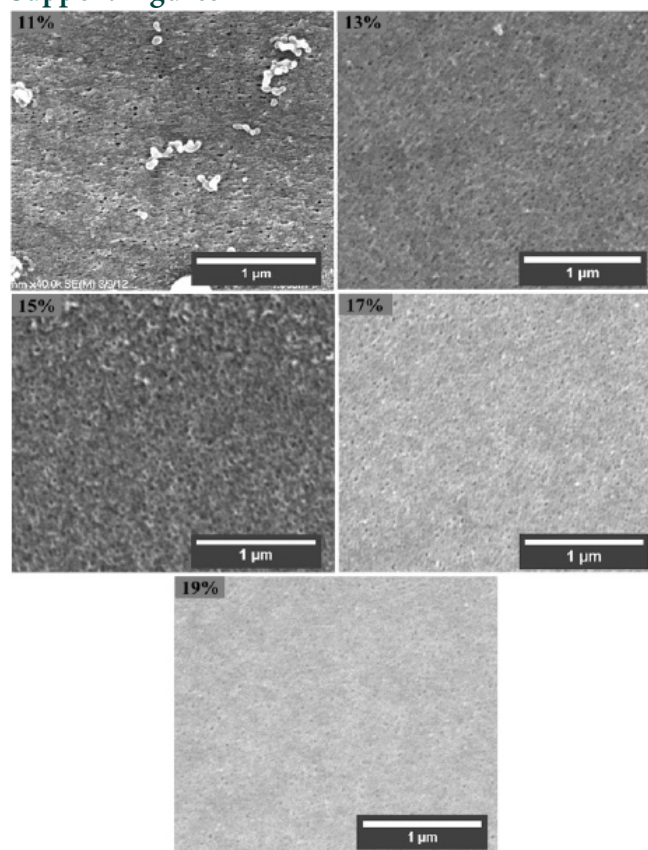


Figure S1: SEM images from surfaces of membranes with different PSf concentrations

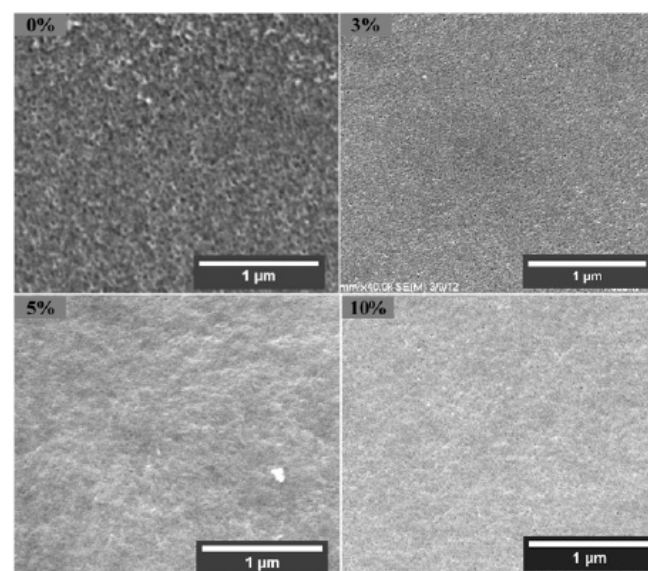


Fig S2: SEM images from surfaces of membranes with different PVP concentrations

Submit your manuscript to a JScholar journal and benefit from:

- ☛ Convenient online submission
- ☛ Rigorous peer review
- ☛ Immediate publication on acceptance
- ☛ Open access: articles freely available online
- ☛ High visibility within the field
- ☛ Better discount for your subsequent articles

Submit your manuscript at  
<http://www.jscholaronline.org/submit-manuscript.php>